PAPER • OPEN ACCESS

Hard x-ray photoelectron spectroscopy on heavy atoms and heavy-element containing molecules using synchrotron radiation up to 35 keV at SPring-8 undulator beamlines

New Journal of Physics
The open access journal at the forefront of physics

Deutsche Physikalische Gesellschaft DPG
IOP Institute of Physics

Published in partnership with: Deutsche Physikalische Gesellschaft and the Institute of Physics

OPEN ACCESS

RECEIVED
12 November 2018

REVISED
23 January 2019

ACCEPTED FOR PUBLICATION
22 February 2019

PUBLISHED
12 April 2019

PAPER

Hard x-ray photoelectron spectroscopy on heavy atoms and heavy-element containing molecules using synchrotron radiation up to 35 keV at SPring-8 undulator beamlines

M Oura[1], **T Gejo**[1,2], **K Nagaya**[1,3], **Y Kohmura**[1], **K Tamasaku**[1], **L Journel**[1,4], **M N Piancastelli**[1,4,5] and **M Simon**[1,4]

[1] RIKEN SPring-8 Center, 1-1-1 Kouto, Sayo-cho, Sayo-gun, Hyogo 679-5148, Japan
[2] Graduate School of Materials Science, University of Hyogo, Kamigori-cho, Ako-gun, Hyogo 678-1297, Japan
[3] Department of Physics, Kyoto University, Kyoto 606-8502, Japan
[4] Sorbonne Université, CNRS, Laboratoire de Chimie Physique-Matière et Rayonnement, LCPMR, F-75005, Paris, France
[5] Department of Physics and Astronomy, Uppsala University, SE-75120 Uppsala, Sweden

E-mail: oura@spring8.or.jp

Keywords: atomic and molecular science, gas-phase HAXPES, hard x-ray undulator radiation

Abstract

We have recently initiated hard x-ray photoelectron spectroscopy experiments on heavy atoms and heavy-element containing molecules in gas phase by using synchrotron radiation up to 35 keV at SPring-8 undulator beamlines. We have successfully measured deep inner-shell photoelectron spectra, as well as L-MM and M-NN Auger electron spectra excited below and above the K-edge of heavy elements. Target specimens utilized for the preliminary experiments are Ar, Kr and Xe atoms, and also iodine in iodomethane (CH_3I) and trifluoroiodomethane (CF_3I) molecules, respectively. We show some selected results on the extracted core-hole lifetime broadenings for the iodine 1s core level of the CH_3I molecule and also for the Xe 2s, 2p core levels, to compare with theoretical values. The L-MM Auger electron spectra of Kr recorded at 13 and 16.6 keV excitation energies are also shown as typical examples, and the spectrum measured above the K-edge, i.e. 14.327 keV, is analyzed based on theoretical calculations using the Hartree–Fock method. As a result, we give a tentative assignment for the double-core-hole hyper-satellite LL-LMM Auger transitions of the Kr atom.

1. Introduction

Hard x-ray photoelectron spectroscopy (HAXPES) at modern synchrotron radiation facilities is widely used nowadays and well known as one of the most powerful methods to directly investigate bulk electronic structure of condensed matter [1], owing to its intrinsic advantages, e.g. surface insensitivity and large probing depth, compared with PES using ultraviolet or soft x-ray radiation. However, similar experimental setups for high-resolution gas-phase experiments, e.g. the resolving power $E/\Delta E$ higher than 5000 (where E is the kinetic energy of electron and ΔE the instrumental resolution), are quite scarce. Up to now, the GALAXIES beamline at the SOLEIL synchrotron [2, 3] has been the only facility for high-resolution HAXPES experiments on atomic and molecular science and has been achieving significant results on double-core-hole spectroscopy [4–7], recoil effects [8–10], ultrafast phenomena [11–13], post-collision interaction (PCI) [14, 15], resonant Auger processes [16–20], and very recent studies on aqueous solution [21, 22]. The experiments at the GALAXIES beamline, however, are limited to the excitation energy ranging between 2.3 and 12 keV, while experiments with much higher photon energy are quite scarce. According to the best of our knowledge, only a few measurements using hard x-rays have been carried out for the deep inner-shell photoelectron spectroscopy on Kr atom and bromine in Br_2 and $BrCF_3$ molecules though the resolving power is about 40 [23, 24].

In 2016, at SPring-8, in order to advance the HAXPES as well as the hard x-ray induced Auger electron spectroscopy experiments on atomic and molecular science by making full use of the characteristic of such a high-energy and high-brilliance x-ray source, we have successfully upgraded an electron spectroscopy apparatus

consisting of a hemispherical analyzer equipped with a gas-cell [25], which enables us to cover the kinetic energy up to 6 keV. Such instrument had been previously utilized to diagnose the characteristics of optics designed for soft x-ray beamlines [26–28] and also to carry out experiments using soft x-ray radiation [29–31]. The purpose of the upgrade has been to be able to perform gas-phase HAXPES experiments at hard x-ray undulator beamlines. In particular, the main objectives are the followings:

- investigation of deep inner-shell photoionization and following decay processes of heavy atoms, e.g. Kr and Xe rare-gas atoms, as well as heavy-element containing molecules, e.g. CH_3SeH, CH_3Br, CH_2BrI, CH_2I_2, CH_3I and CF_3I molecules,
- multi-electron processes, e.g. double-hole states (core–core as well as core-valence) production, to study the dynamics of their excitation/relaxation processes in heavy elements using high-brilliance short x-ray pulses.

Here we would like to stress the novel capabilities of the hard x-ray induced electron spectroscopy gas-phase experiments at the SPring-8 undulator beamline. We are able to apply this method to gain unprecedented insight into a wealth of phenomena concerning deep core levels of heavier element as well as high-energy photoelectrons. Topics in this new area include quantum electrodynamics effects [32], shorter lifetimes, stronger PCI, stronger recoils and so on. For example, we can apply the atomic Auger Doppler effect to study the second-order non-dipole effects [8] by combining with the polarization control technique for the incident photon using the diamond phase retarder [33].

In this paper, we describe briefly the gas-phase HAXPES setup for the hard x-ray induced electron spectroscopy experiments on heavy atoms and heavy-element containing molecules at the SPring-8 undulator beamlines and give some selected examples obtained during the feasibility studies.

2. Experiments

The experimental setup was almost the same as the one described in our recent paper [34]. The apparatus equipped with the hemispherical electron energy analyzer SES-2002 and the gas-cell GC-50 (Scienta Omicron [25]) was used for the measurements of electron spectra. This apparatus is usually installed at the soft x-ray undulator beamline BL17SU [27] (RIKEN beamline) at SPring-8, therefore we move it to the hard x-ray undulator beamline for the gas-phase HAXPES experiments. Feasibility studies were carried out at the RIKEN beamlines BL29XU [35] and BL19LXU [36] of SPring-8.

We have installed the apparatus into the experimental hutch #3 (EH3) at BL29XU and the EH1 at BL19LXU for the atomic and molecular target experiments, respectively. The photon energy ranges covered by these beamlines are 4.4–37.8 keV at BL29XU and 7.2–18 (22–51) keV, where numbers in parenthesis are the energies of 3rd order harmonics of undulator radiation, at BL19LXU, respectively. A monochromatic photon beam in the 6.0–35.5 keV energy range was obtained using a Si(111) double-crystal monochromator cooled by liquid nitrogen [37]. The energy resolutions of the photon beam, i.e. $\Delta E/E$, were about 1.28×10^{-4} (1.27×10^{-4}) 1.35×10^{-4} (1.33×10^{-4}) and 1.64×10^{-4} (1.36×10^{-4}) for 6, 10 and 35 keV, respectively at BL29XU (BL19LXU). The photon beam was collimated using a four-jaw slit to a size of 0.5×0.5 mm^2 before introducing it into the apparatus. Typical photon fluxes were estimated by using an ion chamber to be about 1.7×10^{12} (9.6×10^{13}) at 8 keV and 4.9×10^{12} (7.4×10^{12}) ph s^{-1} at 35.5 keV at BL29XU (BL19LXU), respectively. During the measurement, the target gas pressure was maintained to be about 2×10^{-3} Pa outside the gas-cell. The lens axis of the analyzer was in the horizontal direction at right angles to the photon beam direction and parallel to the polarization vector of the incident photons. The apparatus was mounted on a position-adjustable *XZ*-stage, where *X* stands for the horizontal and *Z* for the vertical directions, respectively, perpendicular to the photon-beam axis, as shown in figure 1.

The energy scale of the incident x-ray beam was calibrated by roughly measuring the Zr K-absorption spectrum and also by precisely recording the 1s photoelectron spectra of several rare-gas atoms to compare with the previously published data [38]. The kinetic energy scales of the electron spectra were calibrated by measuring the Auger electron spectra and the photoelectron spectra of Ar, Kr and Xe atoms. The well-established Ar K-LL and K-LM Auger lines [39] and a Xe L-MM ^{1}G Auger line [40] as well as the L-MM Auger lines of Kr [41] were used as references. In the measurements, the pass energy of the hemispherical analyzer was chosen to be 200 or 500 eV and an appropriate analyzer slit was set to obtain a total energy resolution smaller than the natural linewidth of core-hole states. Thus the resulting energy resolution of the electron analyzer ranged between 0.2 and 3.9 eV. The photon band pass was theoretically calculated to be about 0.84 (4.84) eV at 6.5 (35.5) keV. The thermal Doppler broadening is around several tenth of meV and is negligible for the total experimental broadening as compared to the other contribution. Therefore, the overall resolution for the measurements can be estimated to be about 6.9 eV for the 1s photoelectron spectrum of the Xe atom at 35 keV excitation energy.

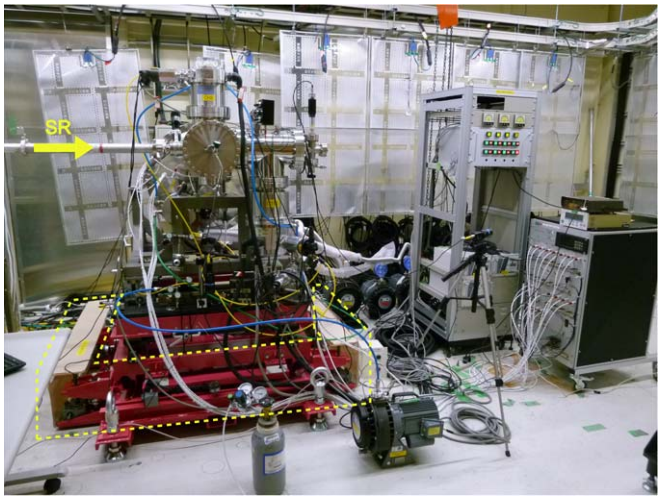

Figure 1. A side-view picture of the gas-phase HAXPES setup installed at the EH3 of BL29XU. The apparatus was mounted on a position-adjustable *XZ*-stage (indicated by the dashed yellow line). The photon beam was coming from the left-hand side (yellow arrow).

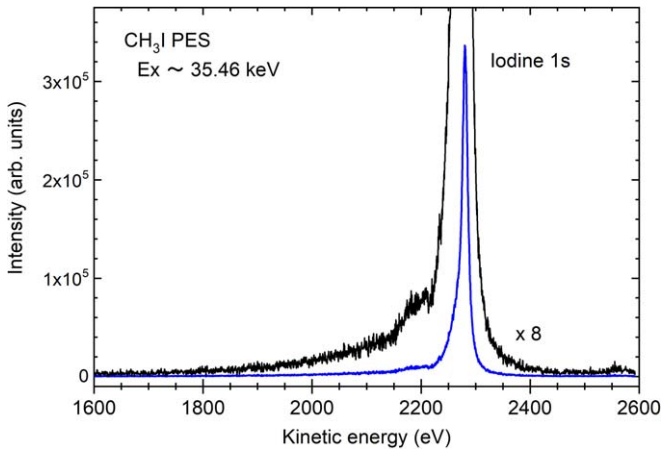

Figure 2. Iodine 1s photoelectron spectrum of the CH_3I molecule measured at a photon energy of 35.46 keV. In addition to the main 1s line at 2281 eV, a weak satellite structure around 2200 eV kinetic energy region is also observed.

3. Results and discussion

3.1. Hard x-ray photoelectron spectroscopy (HAXPES)

The iodine 1s core-level photoelectron spectrum of the CH_3I molecule recorded at a photon energy of 35 455 $\pm$ 5 eV is shown in figure 2. The kinetic energy of the iodine 1s main line is located at 2281 eV. Therefore the iodine 1s binding energy derived from our measurements is 33 174 eV, in fairly good agreement with the literature value of 33 167.2 eV (Exp.) and 33 179.5 eV (Theory) [42]. In addition to the main line, we can recognize a weak bump structure, which can be attributable to the unresolved 5p $\rightarrow$ np ($n = 6, 7, 8, \ldots$) shakeup satellite accompanying the 1s photoionization of iodine in the CH_3I molecule, around 2 200 eV kinetic energy region.

The full width at half maximum (FWHM) of the iodine 1s core-level photoelectron peak can be estimated to be 11.82 $\pm$ 0.36 eV by means of a least-square fitting procedure using four Voigt functions with the same Gaussian width as in the previous Xe 1s case to take account of the satellite structure [34]. In order to achieve a better experimental resolution than the previous Xe 1s case [34], we used a narrower analyzer slit in the present measurement. The electron analyzer resolution with the same setup was independently estimated by measuring the Kr 4p photoemission lines using a well-calibrated soft x-ray radiation at BL17SU before the gas-phase HAXPES experiment. By taking into account the resulting instrumental resolution, i.e. about 4.9 eV, we can extract the iodine 1s core-hole lifetime broadening Γ to be 9.65 $\pm$ 0.43 eV, which corresponds to a lifetime τ of 68 $\pm$ 3 as deduced using the standard formula $\Gamma = \hbar/\tau$. We have also carried out similar measurements on the

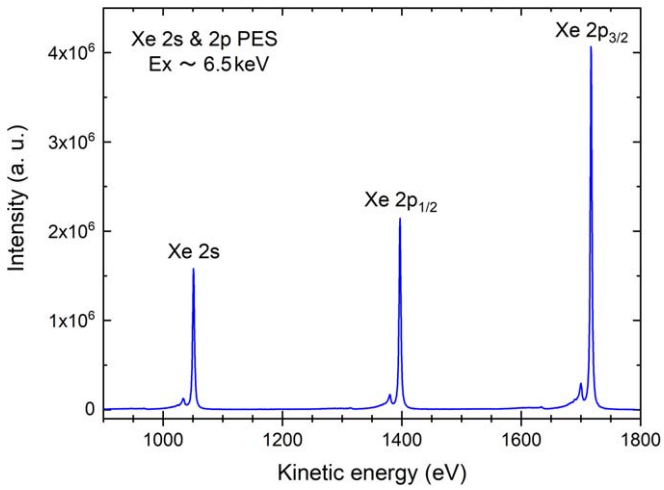

Figure 3. Xenon 2s and 2p photoelectron spectra measured at a photon energy of 6.5 keV. Each line is accompanied by a satellite structure, which is mainly attributable to the 5p → 6p shakeup satellite, on the lower kinetic-energy side tail.

CH_3I and CF_3I molecules with slightly different photon energy, and we have extracted similar values which will be described elsewhere in detail together with the sophisticated theoretical calculations [43]. We notice that the extracted iodine 1s core-hole lifetime is very close to that of the adjacent Xe atom [34]. In the literature [44], the iodine 1s linewidth is reported to be a broader value, i.e. 10.6 eV, and again we could demonstrate a more precise determination of the lifetime of the deep core hole as in the case of Xe atom.

In the fitting procedure, we have tried to incorporate the vibrational progression into the analysis, but we have found that it is hard to extract a reliable result from the fitting, probably due to the very large iodine core-hole lifetime broadening.

In figure 3, we show the xenon 2s and 2p core-level photoelectron spectra measured at a photon energy of 6.5 keV. As can be seen in the figure, we can recognize that each line is accompanied by a satellite structure, which can be mainly attributable to the 5p → 6p shakeup satellite in analogy with the Xe 1s case [34], on the lower kinetic-energy side tail. Similarly, the xenon 2s and 2p photoelectron peaks have been analyzed based on a least-square fitting procedure using Voigt functions with the same Gaussian width, taking into account the experimental resolution (~1.3 eV at 6.5 keV excitation energy) for each peak. The extracted xenon 2s and 2p core-hole lifetime broadenings are given as 2.76 ± 0.07, 2.79 ± 0.04 and 2.60 ± 0.04 eV, for the 2s, $2p_{1/2}$, and $2p_{3/2}$ subshells, respectively. In the previous literature, these are reported to be 3.64, 3.40 and 3.13 eV, for the natural widths of 2s, $2p_{1/2}$ and $2p_{3/2}$, respectively [44], which are close to the values of FWHMs, e.g. 3.30 ± 0.06 (2s), 3.33 ± 0.04 ($2p_{1/2}$) and 3.16 ± 0.04 ($2p_{3/2}$) eV extracted from our analyses. Such fitting procedure also gives an energy difference between the main line and the 5p → 6p shakeup satellite line to be 17.4 eV, which is in fairly good agreement with the value of 5p → 6p shakeup excitation in the case of the Xe 1s line [34].

Figure 4 shows the 1s core-level photoelectron spectra accompanied by the shakeup satellites of (top) Ar, (middle) Kr, and (bottom) Xe atoms. The spectra were recorded at photon energies of 6 (Ar), 20 (Kr) and 35.5 (Xe) keV, respectively. In the Ar spectrum, the shakeup satellites are assigned to be a $1s^{-1}3p^{-1}np$ ($n = 4, 5, 6$) and a $1s^{-1}3s^{-1}ns$ ($n = 4$) series by comparing with the high-resolution x-ray photoabsorption spectrum of the Ar atom near the K-edge [45]. In the Kr spectrum, the shakeup satellites are attributed to a $1s^{-1}4p^{-1}5p$ and a $1s^{-1}4s^{-1}ns$ ($n = 5,6$) series by comparing again with the absorption spectrum of the Kr atom [46]. As can be seen in these spectra, the satellite structure can be well explained by multi-electron excitation processes. In the case of Xe atom, on the other hand, the satellite structure is not clearly resolved from the 1s main line as shown in the figure due to the larger lifetime broadening and also the broader instrumental resolution. We made a bar graph showing the shakeup satellite energies by referring to the calculated energies [34].

It is known that the shakeup or shakeoff probability has a weak excitation energy dependence near the threshold of the single-photon multi-electron excitation processes. Since the first experimental study of the core-level photoemission satellite lines has been performed near a threshold region using synchrotron radiation [47], several experimental studies on rare-gas atoms have been achieved [48–50]. Figure 5 shows the compilation of the experimental data of satellite/main intensity ratio for the Ar 1s case [48–50]. The horizontal axis represents the excess energy, which corresponds to the difference between the incident photon energy and the $1s^{-1}3p^{-1}4p$ binding energy, and the vertical axis indicates the intensity ratio of the $1s^{-1}3p^{-1}4p$ shakeup satellite lines to the main line. The whole previous data essentially indicate a smooth increase and an asymptotic value at higher kinetic energy values, i.e. excess energy of 2 000 eV, of about 9%–10%. Such behavior can be described

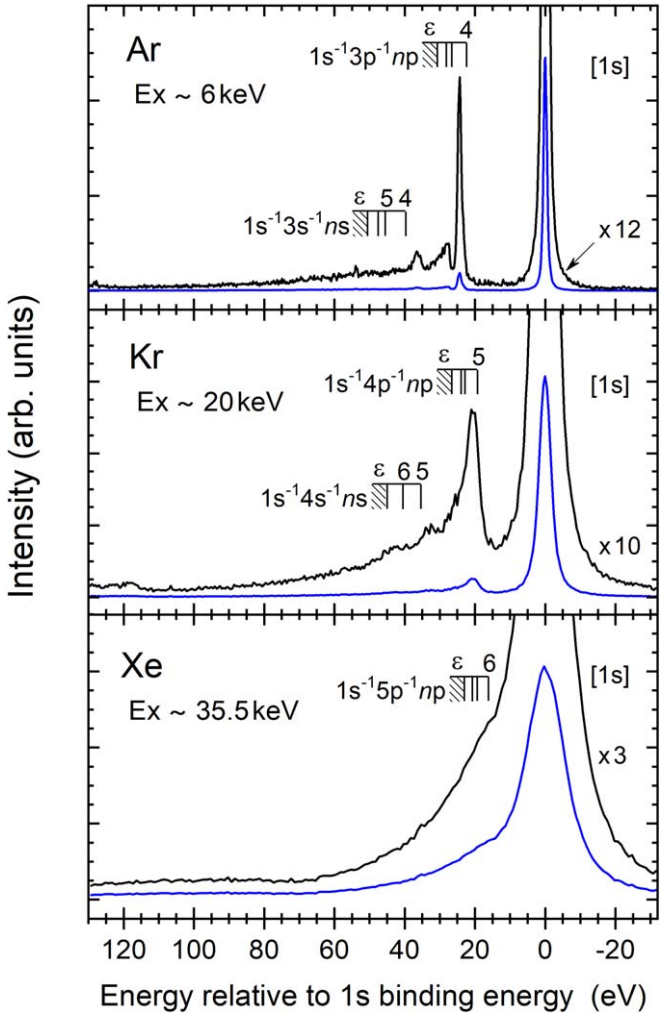

Figure 4. The 1s core-level photoelectron spectra accompanied by the shakeup satellite of (top) Ar, (middle) Kr, and (bottom) Xe atoms. The energies of the shakeup satellites are shown as bar graphs for each element.

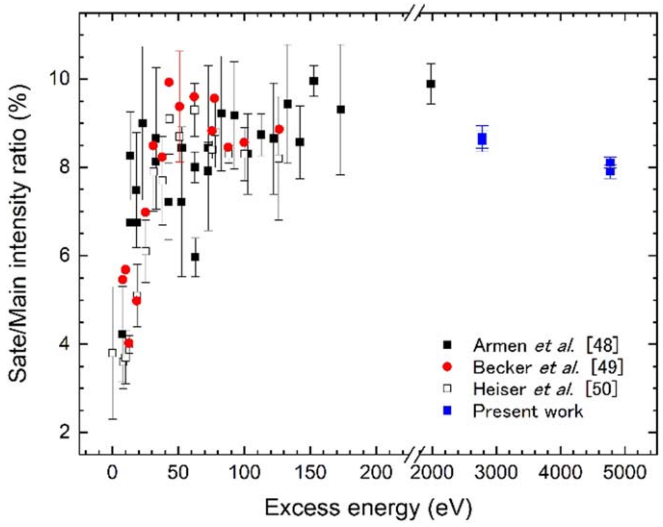

Figure 5. Ratio of the $1s^{-1}3p^{-1}4p$ shakeup satellite line to the main line of Ar as a function of the excess energy, which corresponds to the difference between the incident photon energy and the $1s^{-1}3p^{-1}4p$ binding energy, for the 1 $s^{-1}3p^{-1}4p$ satellite.

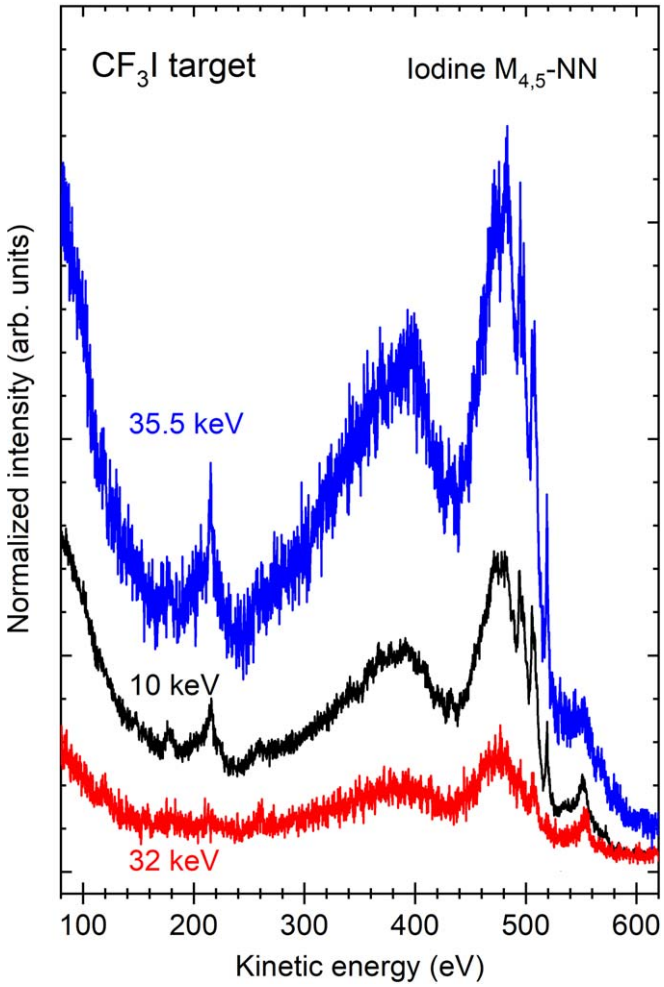

Figure 6. Wide-range spectra of iodine $M_{4,5}$-NN Auger transitions of the CF_3I molecule. The spectra were recorded at photon energies of 10 (black), 32 (red) and 35.5 (blue) keV, respectively. The photon energy of 35.5 keV is above the 1s ionization threshold of iodine, whereas the other two are below threshold. All the spectra were normalized by the accumulation time and the photon flux.

qualitatively by the adiabatic transition model of Thomas [50, 51], which calculates the crossover from the adiabatic to the sudden regime in core ionization and is widely utilized to describe the energy-dependent shake preocesses. Detailed study of such phenomena will give an insight for the intra-atomic electron–electron correlations. Here we measured the Ar 1s core-level photoemission spectra far above the saturation, e.g. at 6 and 8 keV incident photon energies, and extracted the satellite/main intensity ratio as shown in figure 5. At high excess energy, our measurements show the decrease of the intensity ratio. We can continue further such measurements to confirm how the intensity ratio behaves in the high excess energy region, and also we can carry out similar experiments on heavier atom, such as Kr and Xe, in near future.

3.2. Hard x-ray induced Auger electron spectroscopy

The $M_{4,5}$-NN Auger electron spectra of iodine in the CF_3I molecule are shown in figure 6. The spectra were recorded at photon energies of 10 (black), 32 (red) and 35.5 (blue, above the iodine K-edge) keV, respectively. Target gas pressure was maintained to be constant and the analyzer setup was the same during the measurement. All the spectra were normalized by the accumulation time and the photon flux. In all the spectra, two excitation/relaxation channels are available via the direct $M_{4,5}$-shell photoionization followed by the $M_{4,5}$-NN Auger transitions and via the direct L-shell photoionization followed by the L-hole cascading decays leading to the final-step $M_{4,5}$-NN Auger transitions. In the latter case, the L-MM or L-MN Auger transitions produce a relevant fraction of MM or MN multi-vacancy initial states, followed by MM-MNN or MN-MNN Auger transitions. Furthermore, the $L_{1,2}$-hole states easily translate to the $L_{2,3}$-hole state via the fast L_1-$L_{2,3}N$ and L_2-L_3N Coster–Kronig transitions [52] which lead to the satellite $L_{2,3}$N-MMN Auger transitions. On the other hand, in the case of the spectrum excited above the K-edge, i.e. blue curve, additional excitation/relaxation channels involving the cascading K–L–M-hole decay channels are also available. Then there exists a large number of Auger decay channels giving rise to the broad structure of the spectrum. The reduction of spectral

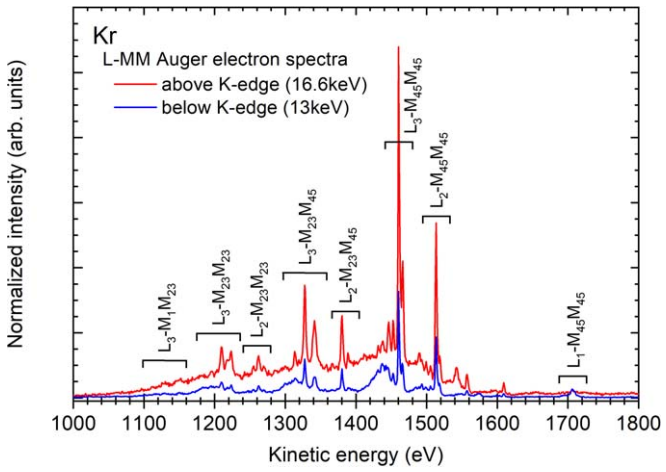

Figure 7. Measured Kr L-MM Auger spectra below (13 keV, blue) and above (16.6 keV, red) the Kr 1s ionization threshold.

intensity from black (10 keV) to red (32 keV) curve is attributable to decrease of the photoionization cross section. The large enhancement in the blue (35.5 keV) curve is due to the edge jump across the K-edge leading to the cascading Auger processes.

In figure 7 we show the wide-range Kr L-MM Auger electron spectra recorded below (13 keV, blue) and above (16.6 keV, red) the Kr 1s ionization threshold. The spectra were normalized by the accumulation time and the photon flux. Detailed assignments for each single L-hole diagram line can be found in the previous literature [41, 53–56] as indicated in the figure, thus we focus our interest on the second-step processes, i.e. double-core-hole hypersatellite LL-LMM Auger transitions following the first-step K-LL Auger transitions which can be observable only in case the excitation energy is above the Kr 1s ionization threshold. A similar discussion for the Xe 1s photoionization is reported in our recent paper [34], but the calculations have revealed that the intensities of second-step LL-LMM Auger transitions of Xe are negligible because the first-step K-LL Auger transitions are much less probable than the K–L x-ray emission, due to the large fluorescence yield, i.e. 0.891 [57], in the Xe atom. We can recognize the large enhancement in the single L-hole diagram lines, e.g. 1 460.2 and 1 513.2 eV, in the spectrum excited above the K-edge. This is attributable to the single L-hole $L_{2,3}$-MM Auger transitions following the first-step K–L x-ray emission.

The pronounced peak, i.e. 1 460 eV, is accompanied by some sharp satellites on the lower kinetic energy side, probably due to the LM-MMM or LN-MMN satellite Auger transitions following the first-step K-LM or K-LN Auger transitions. On the other hand, we notice that there are some broad peaks only in the spectrum excited above the K-edge. The typical case is the broad peak around 1542 eV. This line is definitely broader than the other diagram lines. We can expect this broad peak originated by the double-core-hole hypersatellite LL-LMM Auger transitions.

In order to interpret the excitation/relaxation properties for the double-core-hole hypersatellite LL-LMM Auger transitions, we have simply carried out atomic-structure calculations to obtain an energy diagram of the ground, excited and relaxed states of the neutral Kr as well as the Kr ions based on the multi-configuration Dirac-Fock calculation code [58]. Figure 8 schematically shows the calculated energy diagram for the Kr–Kr^{4+}, although the vertical scale does not give us correct energies. In fact, there are numerous energy levels, therefore we have drawn only the typical electronic configurations and the representative excitation/relaxation channels. As we see in figure 8, the double-core-hole hypersatellite LL-LMM Auger transitions are available only following the double L-hole production by K-LL Auger transitions. If the excitation energy is above the thresholds of double L-hole production, i.e. 3.48 keV, as can be roughly estimated based on the $Z + 1$ approximation, the direct double L-hole photoionization phenomena due to shake processes are also open channels, but we may expect that those are much less probable compared to the processes via the K-LL $\Rightarrow$ LL-LMM cascading pathways.

We have mainly calculated energies and also transition rates for the single L-hole L-MM Auger spectrum as well as the double L-hole hypersatellite LL-LMM Auger spectrum to understand the measured one excited above the K-edge. We focused our interest on the LL-LMM double L-hole hypersatellite, thus we did not calculate here the LM-MMM or LN-MMN satellite Auger transitions. Initial numbers of hole states in K-shell and L_i-subshells ($i = 1, 2, 3$) were estimated by using the tabulated theoretical photoionization cross sections [59]. The calculations were simply made based on the Hartree–Fock approximation using Cowan's code [60]. As a result, the theoretical calculations give us transitions at 1490 and 1542 eV, which are very close to the observed broad

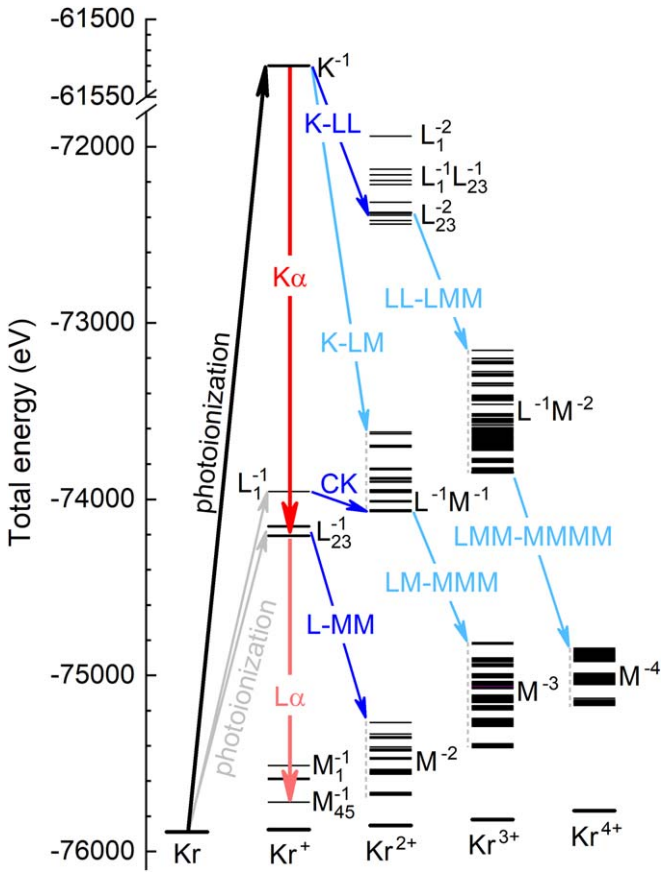

Figure 8. Calculated energy diagram of the ground, excited and relaxed states of the neutral Kr as well as the Kr ions together with their decay properties. Typical excitation/relaxation channels are shown as arrows. Kα (Lα): Kα (Lα) x-ray emission, CK: Coster–Kronig transitions, K-LM: Auger transition from K^{-1} state to L^{-1} M^{-1} state, and so on.

peaks shown in figure 7. Therefore, we tentatively assign these peaks as originating from the double $L_{2,3}$-hole hypersatellite Auger transitions. More detailed sophisticated calculations will be given elsewhere in near future [61].

4. Summary

In this article, we describe the gas-phase electron spectroscopy apparatus recently upgraded for the HAXPES experiments on heavier elements using synchrotron radiation up to 35 keV at SPring-8 undulator beamlines. We have successfully demonstrated the feasibility of the method and given some selected results on iodine in the CH_3I and CF_3I molecules as well as on Kr and Xe atoms showing the capability of the experiments at SPring-8 to investigate the deep core-levels. At the moment, gas-phase experiments in the hard x-ray region higher than 12 keV are feasible only at SPring-8 undulator beamline. The present apparatus can be also used for experiments at the soft x-ray beamlines as well as at the x-ray free-electron laser facility, SACLA.

Acknowledgments

The synchrotron radiation experiments were performed at BL29XU and BL19LXU of SPring-8 with the approval of RIKEN SPring-8 Center (proposals nos. 20160025 and 20170028). We would like to thank TOSO F-TECH, Inc. for providing CF_3I samples. The authors are grateful to the member of the Engineering Team of the RIKEN SPring-8 Center for their technical assistance.

ORCID iDs

L Journel https://orcid.org/0000-0001-8044-5437

References

[1] Woicik J C (ed) 2016 *Hard X-ray Photoelectron Spectroscopy (HAXPES)* (Switzerland: Springer International Publishing)
[2] Céolin D *et al* 2013 Hard x-ray photoelectron spectroscopy on the GALAXIES beamline at the SOLEIL synchrotron *J. Electron Spectrosc. Relat. Phenom.* **190** 188
[3] Rueff J-P, Ablett J M, Céolin D, Priuer D, Moreno Th, Balédent V, Lassalle-Kaiser B, Rault J E, Simon M and Shukla A 2015 The GALAXIES beamline at the SOLEIL synchrotron: inelastic x-ray scattering and photoelectron spectroscopy in the hard x-ray range *J. Synchrotron Radiat.* **22** 175
[4] Püttner R *et al* 2015 Direct observation of double-core-hole shake-up states in photoemission *Phys. Rev. Lett.* **114** 093001
[5] Carniato S *et al* 2016 Photon-energy dependence of single-photon simultaneous core ionization and core excitation in CO_2 *Phys. Rev.* A **94** 013416
[6] Goldsztejn G *et al* 2016 Double-core-hole states in neon: lifetime, post-collision interaction, and spectral assignment *Phys. Rev. Lett.* **117** 133001
[7] Goldsztejn G *et al* 2017 Experimental and theoretical study of the double-core-hole hypersatellite Auger spectrum of Ne *Phys. Rev.* A **96** 012513
[8] Simon M *et al* 2014 Atomic Auger Doppler effects upon emission of fast photoelectrons *Nat. Commun.* **5** 4069
[9] Kukk E *et al* 2017 Photoelectron recoil in CO in the x-ray region up to 7 keV *Phys. Rev.* A **95** 042509
[10] Kukk E *et al* 2018 Energy transfer into molecular vibrations and rotations by recoil in inner-shell photoemission *Phys. Rev. Lett.* **121** 073002
[11] Piancastelli M N, Goldsztejn G, Marchenko T, Guillemin R, Kushawaha R K, Journel L, Carniato S, Rueff J-P, Céolin D and Simon M 2014 Core-hole-clock spectroscopies in the tender x-ray domain *J. Phys. B: At. Mol. Opt. Phys.* **47** 124031
[12] Travnikova O *et al* 2016 Hard-x-ray-induced multistep ultrafast dissociation *Phys. Rev. Lett.* **116** 213001
[13] Travnikova O *et al* 2017 Subfemtosecond control of molecular fragmentation by hard x-ray photons *Phys. Rev. Lett.* **118** 213001
[14] Guillemin R, Sheinerman S, Bomme C, Journel L, Marin T, Marchenko T, Kushawaha R K, Trcera N, Piancastelli M N and Simon M 2012 Ultrafast dynamics in postcollision interaction after multiple Auger decays in argon 1s photoionization *Phys. Rev. Lett.* **109** 013001
[15] Guillemin R, Sheinerman S, Püttner R, Marchenko T, Goldsztejn G, Journel L, Kushawaha R K, Céolin D, Piancastelli M N and Simon M 2015 Postcollision interaction effects in KLL Auger spectra following argon 1s photoionization *Phys. Rev.* A **92** 012503
[16] Céolin D *et al* 2015 Auger resonant-Raman study at the Ar K edge as probe of electronic-state-lifetime interferences *Phys. Rev.* A **91** 022502
[17] Kushawaha R K *et al* 2015 Auger resonant-Raman decay after Xe L-edge photoionization *Phys. Rev.* A **92** 013427
[18] Goldsztejn G, Marchenko T, Céolin D, Journel L, Guillemin R, Rueff J-P, Kushawaha R K, Püttner R, Piancastelli M N and Simon M 2016 Electronic state-lifetime interference in resonant Auger spectra: a tool to disentangle overlapping core-excited states *Phys. Chem. Chem. Phys.* **18** 15133
[19] Goldsztejn G *et al* 2017 Electronic-state-lifetime interference in the hard-x-ray regime: argon as a showcase *Phys. Rev.* A **95** 012509
[20] Püttner R *et al* 2017 Detailed assignment of normal and resonant Auger spectra of Xe near the L edges *Phys. Rev.* A **96** 022501
[21] Céolin D *et al* 2017 Ultrafast charge transfer processes accompanying KLL Auger decay in aqueous KCl solution *Phys. Rev. Lett.* **119** 263003
[22] Miteva T *et al* 2018 The all-seeing eye of resonant Auger electron spectroscopy: a study on aqueous solution using tender x-rays *J. Phys. Chem. Lett.* **9** 4457
[23] Krässig B, Bilheux J-C, Dunford R W, Gemmell D S, Hasegawa S, Kanter E P, Southworth S H and Young L 2003 Nondipole asymmetries of Kr 1s photoelectrons *Phys. Rev.* A **67** 022707
[24] Southworth S H, Dunford R W, Kanter E P, Krässig B, Young L, LaJohn L A and Pratt R H 2006 Nondipole asymmetries of K-shell photoelectrons of Kr, Br_2, and $BrCF_3$ *Rad. Phys. Chem.* **75** 1574
[25] The analyzer as well as the gas-cell were originally supplied by Gammadata Scienta. Present company name is ScientaOmicron.
[26] Ohashi H, Senba Y, Ishiguro E, Goto S, Shin S and Ishikawa T 2006 Evaluation of a modern soft x-ray monochromator with high resolving power over 10000 *Proc. SPIE* **6317** 63171A
[27] Ohashi H *et al* 2007 Performance of a highly stabilized and high-resolution beamline BL17SU for advanced soft x-ray spectroscopy at SPring-8 *AIP Conf. Proc.* **879** 523
[28] Senba Y, Ohashi H, Kishimoto H, Miura T, Goto S, Shin S, Shintake T and Ishikawa T 2007 Fundamental techniques for high photon energy stability of a modern soft x-ray beamline *AIP Conf. Proc.* **879** 718
[29] Oura M, Senba Y and Ohashi H 2008 Resonant enhancement of photoemission leading to the Ne^+ $[2p^2](^1D)3p\ ^2P$ state across the $[1s2p](^3P)3p^2\ ^1P$ double-excitation resonance of Ne *Phys. Rev.* A **77** 054702
[30] Gejo T, Oura M, Kuniwake M, Honma K and Harries J R 2011 Dissociation and recapture dynamics in H_2O following O 1s inner-shell excitation *J. Phys.: Conf. Ser.* **288** 012023
[31] Gejo T, Oura M, Tokushima T, Horikawa Y, Arai H, Shin S, Kimberg V and Kosugi N 2017 Resonant inelastic x-ray scattering and photoemission measurement of O_2: direct evidence for dependence of Rydberg-valence mixing on vibrational states in O 1s $\rightarrow$ Rydberg states *J. Chem. Phys.* **147** 044310
[32] Niskanen J, Jänkälä K, Huttula M and Föhlisch A 2017 QED effects in 1s and 2s single and double ionization potentials of the noble gases *J. Chem. Phys.* **146** 144312
[33] Maruyama H *et al* 1999 Polarization tunability and analysis for observing magnetic effects on BL39XU at SPring-8 *J. Synchrotron Radiat.* **6** 1133
[34] Piancastelli M N, Jänkälä K, Journel L, Gejo T, Kohmura Y, Huttula M, Simon M and Oura M 2017 X-ray versus Auger emission following Xe 1s photoionization *Phys. Rev.* A **95** 061402 (R)
[35] Tamasaku K, Tanaka Y, Yabashi M, Yamazaki H, Kawamura N, Suzuki M and Ishikawa T 2001 SPring-8 RIKEN beamline III for coherent x-ray optics *Nucl. Instrum. Methods* A **467-468** 686
[36] Yabashi M *et al* 2001 Design of a beamline for the SPring-8 long undulator source 1 *Nucl. Instrum. Methods* A **467–468** 678
[37] Mochizuki T, Kohmura Y, Awaji A, Suzuki Y, Baron A, Tamasaku K, Yabashi M, Yamazaki H and Ishikawa T 2001 Cryogenic cooling monochromators for the SPring-8 undulator beamlines *Nucl. Instrum. Methods* A **467–468** 647
[38] Breinig M, Chen M H, Ice G E, Parente F and Crasemann B 1980 Atomic inner-shell level energies determined by absorption spectrometry with synchrotron radiation *Phys. Rev.* A **22** 520
[39] Asplund L, Kelfve P, Bomster B, Siegbahn H and Siegbahn K 1977 Argon KLL and KLM Auger electron spectra *Phys. Scr.* **16** 268
[40] Armen G B, Åberg T, Levin J C, Crasemann B, Chen M H, Ice G E and Brown G S 1985 Threshold excitation of short-lived atomic inner-shell hole states with synchrotron radiation *Phys. Rev. Lett.* **54** 1142

[41] Levin J C, Sorensen S L, Crasemann B, Chen M H and Brown G S 1986 Krypton L-MM Auger spectra: new measurements and analysis *Phys. Rev.* A **33** 968
[42] Deslattes R D, Kessler E G Jr, Indelicato P, de Billy L, Lindroth E and Anton J 2003 X-ray transition energies: new approach to a comprehensive evaluation *Rev. Mod. Phys.* **75** 35
[43] Boudjemia N, Jänkälä K, Gejo T, Nagaya K, Tamasaku K, Huttula M, Piancastelli M N, Simon M and Oura M 2019 Deep core photoionization of iodine in CH_3I and CF_3I molecules: how deep down does the chemical shift reach? *Phys. Chem. Chem. Phys.* **21** 5448–54
[44] Krause M O 1979 Natural widths of atomic K and L levels, Kα x-ray lines and several KLL Auger lines *J. Phys. Chem. Ref. Data* **8** 329
[45] Deutsch M, Maskil N and Drube W 1992 Multielectronic excitations near the K edge of argon *Phys. Rev.* A **46** 3963
[46] Deutsch M and Hart M 1986 Multielectron x-ray photoexcitation measurements in krypton *Phys. Rev. Lett.* **57** 1566
[47] Kobrin P H, Southworth S, Truesdale C M, Lindle D W, Becker U and Shirley D A 1984 Threshold measurements of the K-shell photoelectron satellites in Ne and Ar *Phys. Rev.* A **29** 194
[48] Armen G B, Åberg T, Karim K R, Levin J C, Crasemann B, Brown G S, Chen M H and Ice G E 1985 Threshold double photoexcitation of argon with synchrotron radiation *Phys. Rev. Lett.* **54** 182
[49] Becker U and Shirley D A 1990 Threshold behavior and resonances in the photoionization of atoms and molecules *Phys. Scr.* **T31** 56
[50] Heiser F, Whitfield S B, Viefhaus J, Becker U, Heimann P A and Shirley D A 1994 Threshold and near-threshold photoelectron spectroscopy around the Ar K edge *J. Phys. B: At. Mol. Opt. Phys.* **27** 19
[51] Thomas T D 1984 Transition from adiabatic to sudden excitation of core electrons *Phys. Rev. Lett.* **52** 417
[52] Chen M H, Crasemann B and Mark H 1979 Relativistic radiationless transition probabilities for atomic K- and L-shells *At. Data Nucl. Data Tables* **24** 13
[53] Krause M O 1965 Relative intensities of prominent LMM Auger transitions in krypton *Phys. Lett.* **19** 14
[54] Siegbahn K *et al* 1971 *ESCA Applied to Free Molecules* (Amsterdam: North-Holland Publishing Company)
[55] Werme L O, Bergmark T and Siegbahn K 1972 The high resolution $L_{2,3}MM$ and $M_{4,5}NN$ Auger spectra from krypton and $M_{4,5}NN$ and $N_{4,5}OO$ Auger spectra from xenon *Phys. Scr.* **6** 141
[56] Aksela H, Aksela S, Väyrynen J and Thomas T D 1980 $L_{2,3}M_{4,5}X$ Auger electron spectra of Br_2 and Kr: anomalous $L_2M_{2,3}M_{4,5}$ spectra *Phys. Rev.* A **22** 1116
[57] Krause M O 1979 Atomic radiative and radiationless yields for K and L shells *J. Phys. Chem. Ref. Data* **8** 307
[58] Dyall K G, Grant I P, Johnson C T, Parpia F A and Plummer E P 1989 GRASP: a general-purpose relativistic atomic structure program *Comput. Phys. Commun.* **55** 425
[59] Scofield J H 1973 *Theoretical photoionization cross sections from 1 to 1500 keV* UCRL-51326 Lowrence Livermore Laboratory
[60] Cowan R D 1981 *The Theory of Atomic Structure and Spectra* (Berkeley: University of California Press)
[61] Boudjemia N *et al* to be submitted